

Supporting Information for

Meso-2'-Linked Porphyrin-BODIPY Hybrids: Synthesis and Efficient Excitation Energy Transfer

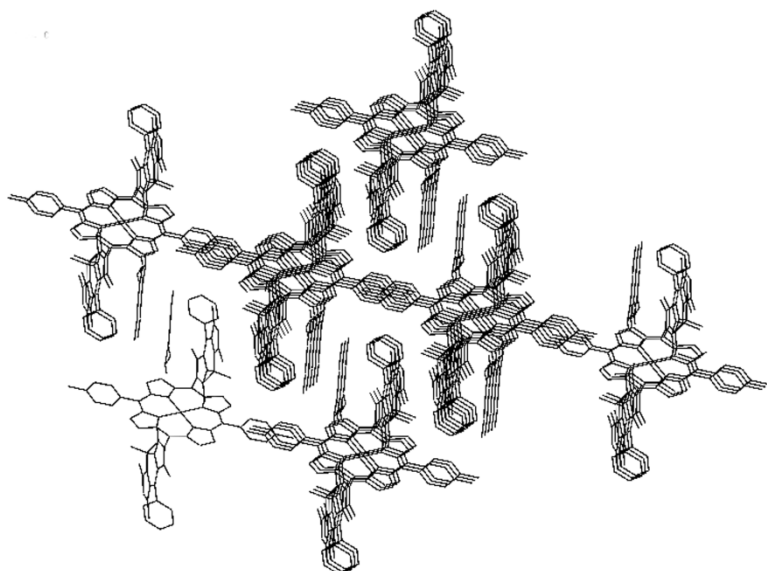
Qin-Qin Hu, Yi-Zhou Zhu, Shao-chun Zhang, Yu-Zhang Tong, Jian-Yu Zheng**

State Key Laboratory and Institute of Elemento-Organic Chemistry, Collaborative Innovation Center of Chemical Science and Engineering (Tianjin), Nankai University, Tianjin 300071, China

E-mail: jyzheng@nankai.edu.cn, zhuyizhou@nankai.edu.cn.

Table S1 Crystal data and refinement details

Compound reference	2BDP-ZnP
Chemical formula	C79.25 H74.25 B2 Cl0.75 F4 N8 Zn
Formula Mass	1328.29
Crystal system	Triclinic
<i>a</i> /Å	9.964(2)
<i>b</i> /Å	14.138(4)
<i>c</i> /Å	14.813(4)
α /°	112.246(5)
β /°	103.109(3)
γ /°	95.620(4)
Unit cell volume/Å ³	1841.6(8)
Temperature/K	113(2)
Space group	<i>P</i> Error!
No. of formula units per unit cell, <i>Z</i>	1
Radiation type	MoK\α
Absorption coefficient, μ/mm^{-1}	0.418
No. of reflections measured	23127
No. of independent reflections	83004
R_{int}	0.0344
Final R_I values ($I > 2\sigma(I)$)	0.0646
Final $wR(F^2)$ values ($I > 2\sigma(I)$)	0.2072
Final R_I values (all data)	0.0764
Final $wR(F^2)$ values (all data)	0.2072
Goodness of fit on F^2	1.109

**Fig. S1** Packing diagram of the hybrid **2BDP-ZnP**. The hydrogen atoms are omitted for clarity.**Table S2** Bond lengths and bond angles

Bond lengths			
Zn(1)-N(2)#1	2.032(2)	C(14)-C(15)	1.450(4)
Zn(1)-N(2)	2.032(2)	C(15)-C(16)	1.353(4)
Zn(1)-N(1)	2.039(2)	C(16)-C(17)	1.442(4)
Zn(1)-N(1)#1	2.039(2)	C(17)-C(8)#1	1.400(4)
F(1)-B(1)	1.382(4)	C(18)-C(19)	1.391(4)
F(2)-B(1)	1.388(4)	C(18)-C(22)	1.408(4)
N(1)-C(9)	1.369(4)	C(19)-C(21)	1.432(4)
N(1)-C(12)	1.375(4)	C(19)-C(20)	1.498(4)
N(2)-C(17)	1.371(4)	C(21)-C(24)	1.406(4)
N(2)-C(14)	1.372(4)	C(22)-C(23)	1.494(4)
N(3)-C(22)	1.350(4)	C(24)-C(31)	1.386(4)
N(3)-C(21)	1.390(4)	C(24)-C(25)	1.491(4)
N(3)-B(1)	1.553(4)	C(25)-C(26)	1.387(6)
N(4)-C(35)	1.347(4)	C(25)-C(30)	1.392(5)
N(4)-C(31)	1.404(4)	C(26)-C(27)	1.395(6)
N(4)-B(1)	1.550(4)	C(27)-C(28)	1.381(9)
C(1)-C(2)	1.510(5)	C(28)-C(29)	1.361(9)
C(2)-C(3)	1.372(5)	C(29)-C(30)	1.389(6)
C(2)-C(7)	1.386(5)	C(31)-C(32)	1.436(4)
C(3)-C(4)	1.393(5)	C(32)-C(34)	1.382(5)
C(4)-C(5)	1.376(5)	C(32)-C(33)	1.492(5)
C(5)-C(6)	1.378(5)	C(34)-C(35)	1.406(5)
C(5)-C(8)	1.505(4)	C(35)-C(36)	1.479(5)
C(6)-C(7)	1.390(5)	C(37)-C(38)	1.527(7)
C(8)-C(9)	1.399(4)	C(38)-C(39)	1.474(7)
C(8)-C(17)#1	1.400(4)	C(39)-C(40)	1.496(6)
C(9)-C(10)	1.443(4)	C(40)-C(41)	1.500(7)
C(10)-C(11)	1.343(4)	C(41)-C(42)	1.505(8)
C(11)-C(12)	1.443(4)	C(42)-C(43)	1.521(8)
C(12)-C(13)	1.399(4)	C(1)-C(44)	1.713(10)
C(13)-C(14)	1.402(4)	C(2)-C(44)	1.722(10)
C(13)-C(18)	1.490(4)	C(3)-C(44)	1.724(10)
Bond angles			
N(2)#1-Zn(1)-N(2)	180	N(2)-C(14)-C(13)	126.1(3)
N(2)#1-Zn(1)-N(1)	90.70(10)	N(2)-C(14)-C(15)	109.4(3)
N(2)-Zn(1)-N(1)	89.30(10)	C(13)-C(14)-C(15)	124.4(3)
N(2)#1-Zn(1)-N(1)#1	89.30(10)	C(16)-C(15)-C(14)	107.1(3)
N(2)-Zn(1)-N(1)#1	90.70(10)	C(15)-C(16)-C(17)	107.1(3)
N(1)-Zn(1)-N(1)#1	180	N(2)-C(17)-C(8)#1	125.8(3)
C(9)-N(1)-C(12)	106.4(2)	N(2)-C(17)-C(16)	109.8(3)
C(9)-N(1)-Zn(1)	126.1(2)	C(8)#1-C(17)-C(16)	124.4(3)
C(12)-N(1)-Zn(1)	127.54(19)	C(19)-C(18)-C(22)	108.0(3)

C(17)-N(2)-C(14)	106.7(2)	C(19)-C(18)-C(13)	127.0(3)
C(17)-N(2)-Zn(1)	125.99(19)	C(22)-C(18)-C(13)	124.9(3)
C(14)-N(2)-Zn(1)	127.12(19)	C(18)-C(19)-C(21)	106.1(3)
C(22)-N(3)-C(21)	108.5(2)	C(18)-C(19)-C(20)	125.5(3)
C(22)-N(3)-B(1)	125.8(3)	C(21)-C(19)-C(20)	128.4(3)
C(21)-N(3)-B(1)	125.6(2)	N(3)-C(21)-C(24)	120.6(3)
C(35)-N(4)-C(31)	108.6(3)	N(3)-C(21)-C(19)	108.1(2)
C(35)-N(4)-B(1)	125.7(3)	C(24)-C(21)-C(19)	131.3(3)
C(31)-N(4)-B(1)	125.6(3)	N(3)-C(22)-C(18)	109.3(3)
F(1)-B(1)-F(2)	109.9(3)	N(3)-C(22)-C(23)	122.7(3)
F(1)-B(1)-N(4)	110.1(3)	C(18)-C(22)-C(23)	128.1(3)
F(2)-B(1)-N(4)	110.3(3)	C(31)-C(24)-C(21)	120.8(3)
F(1)-B(1)-N(3)	110.7(3)	C(31)-C(24)-C(25)	120.4(3)
F(2)-B(1)-N(3)	109.8(3)	C(21)-C(24)-C(25)	118.7(3)
N(4)-B(1)-N(3)	105.9(3)	C(26)-C(25)-C(30)	120.2(4)
C(3)-C(2)-C(7)	117.3(3)	C(26)-C(25)-C(24)	121.0(3)
C(3)-C(2)-C(1)	121.1(3)	C(30)-C(25)-C(24)	118.8(3)
C(7)-C(2)-C(1)	121.6(3)	C(25)-C(26)-C(27)	119.4(5)
C(2)-C(3)-C(4)	121.7(3)	C(28)-C(27)-C(26)	119.7(5)
C(5)-C(4)-C(3)	120.4(3)	C(29)-C(28)-C(27)	120.8(4)
C(4)-C(5)-C(6)	118.8(3)	C(28)-C(29)-C(30)	120.6(5)
C(4)-C(5)-C(8)	121.2(3)	C(29)-C(30)-C(25)	119.3(5)
C(6)-C(5)-C(8)	120.0(3)	C(24)-C(31)-N(4)	120.5(3)
C(5)-C(6)-C(7)	120.2(3)	C(24)-C(31)-C(32)	132.0(3)
C(2)-C(7)-C(6)	121.6(3)	N(4)-C(31)-C(32)	107.5(3)
C(9)-C(8)-C(17)#1	125.6(3)	C(34)-C(32)-C(31)	106.2(3)
C(9)-C(8)-C(5)	117.3(3)	C(34)-C(32)-C(33)	125.0(3)
C(17)#1-C(8)-C(5)	117.2(3)	C(31)-C(32)-C(33)	128.9(3)
N(1)-C(9)-C(8)	125.6(3)	C(32)-C(34)-C(35)	108.7(3)
N(1)-C(9)-C(10)	109.6(3)	N(4)-C(35)-C(34)	109.1(3)
C(8)-C(9)-C(10)	124.7(3)	N(4)-C(35)-C(36)	122.6(3)
C(11)-C(10)-C(9)	107.4(3)	C(34)-C(35)-C(36)	128.4(3)
C(10)-C(11)-C(12)	107.0(3)	C(39)-C(38)-C(37)	115.1(6)
N(1)-C(12)-C(13)	125.3(3)	C(38)-C(39)-C(40)	118.5(5)
N(1)-C(12)-C(11)	109.6(2)	C(39)-C(40)-C(41)	116.3(6)
C(13)-C(12)-C(11)	125.1(3)	C(40)-C(41)-C(42)	115.3(6)
C(12)-C(13)-C(14)	124.5(3)	C(41)-C(42)-C(43)	113.5(7)
C(12)-C(13)-C(18)	118.4(3)	Cl(1)-C(44)-Cl(2)	114.6(8)
C(14)-C(13)-C(18)	117.0(2)	Cl(1)-C(44)-Cl(3)	115.0(8)
N(2)#1-Zn(1)-N(2)	180		

Symmetry transformations used to generate equivalent atoms: #1 -x,-y+1,-z

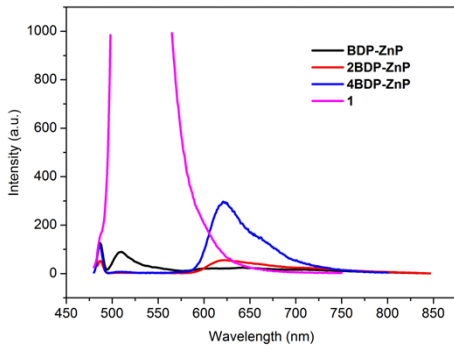
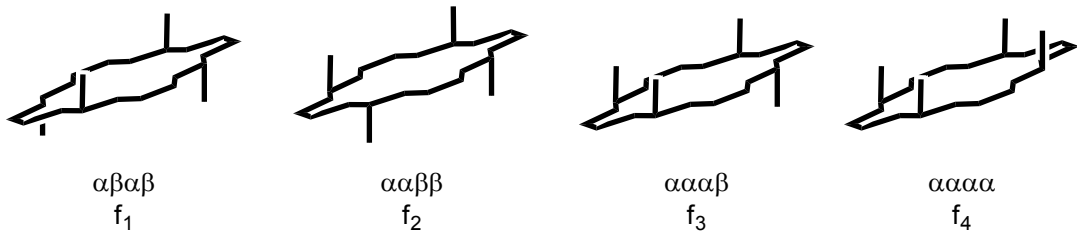


Fig. S2 Fluorescence spectra of **BDP-ZnP** (black), **2BDP-ZnP** (red), **4BDP-ZnP** (blue), and compound **1** (magenta) in CHCl_3 ($\lambda_{\text{ex}} = 488 \text{ nm}$). All the absorptions of hybrid samples were normalized at 488 nm.



Scheme S1 Diagrammatic representation of the atropisomers (α means the phenyl group of BODIPY units up; β down).

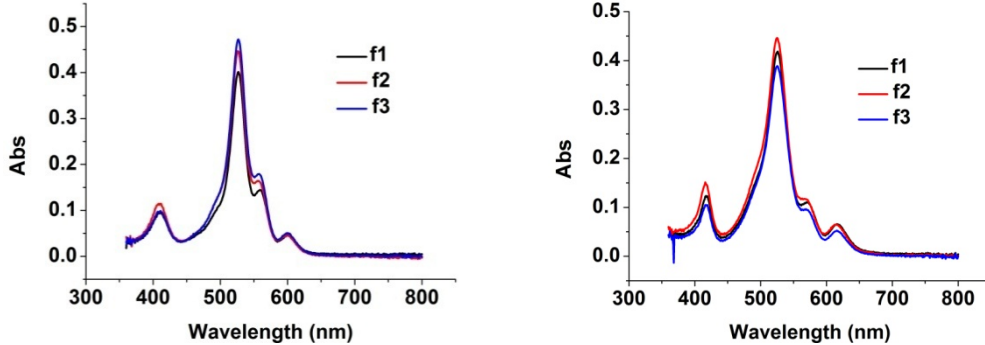


Fig. S3 UV-visible spectra of the **4BDP-ZnP** atropisomers in CHCl_3 (left) and in DMF (right).

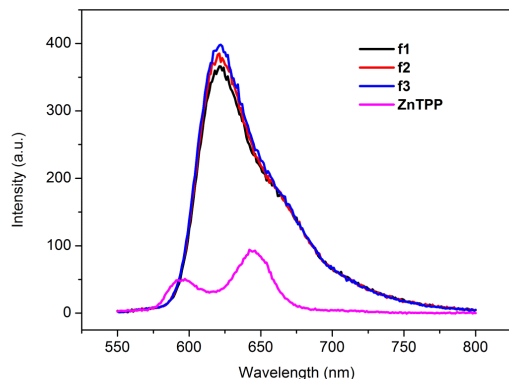


Fig. S4 Fluorescence spectra of the **4BDP-ZnP** atropisomers f_1 (black), f_2 (red), f_3 (blue), and the

reference **ZnTPP** (magenta) in toluene ($\lambda_{\text{ex}} = 540 \text{ nm}$). All the measured atropisomer samples and the reference **ZnTPP** sample had equal absorption intensity at 540 nm.

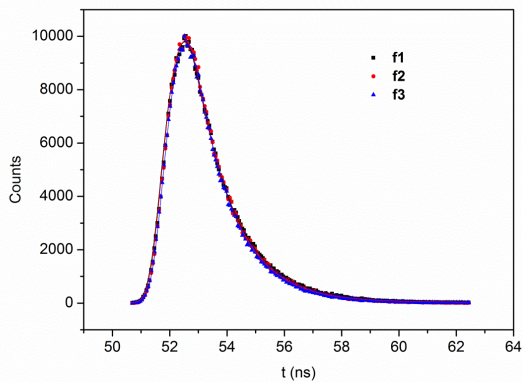


Fig. S5 Fluorescence decays of the **4BDP-ZnP** atropisomers **f1** (black), **f2** (red), and **f3** (blue) measured at the emission wavelength of the Zn porphyrin moiety (630 nm) in toluene (The pump wavelength is 450 nm).

According to the reported cases, three fractions can usually be separated, and the fourth fraction with the biggest polarity can be obtained by further interconversion later.^{1,2} Similar to that, only three fractions were obtained in our case. After metallation with zinc acetate, we got the corresponding metalloporphyrins. The three **4BDP-ZnP** isomers exhibit almost identical UV-visible spectra either in CHCl_3 or in DMF in Figure S3.^{3,4} At the same time, in our experiments, all the atropisomers have the nearly same emission spectra (Fig. S4) and the fluorescence decay (Fig. S5). As shown in Figure S6, the β -H of $\alpha\beta\alpha\beta$ -**4BDP-ZnP** shows single peak, while the $\alpha\alpha\beta\beta$ - and $\alpha\alpha\alpha\beta$ -**4BDP-ZnP** present double peaks.

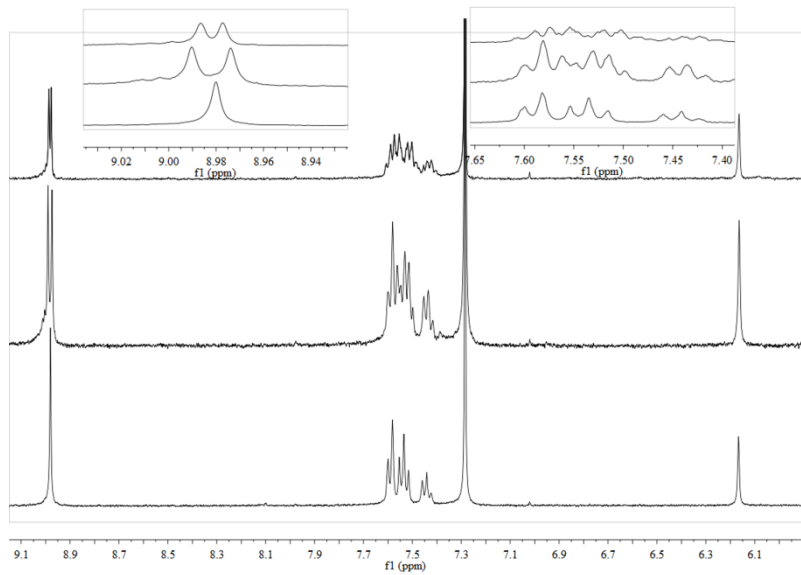


Fig. S6 ^1H NMR spectra for the hybrids **4BDP-ZnP** in CDCl_3 (top) **f₃**, (center) **f₂**, and (bottom) **f₁**.

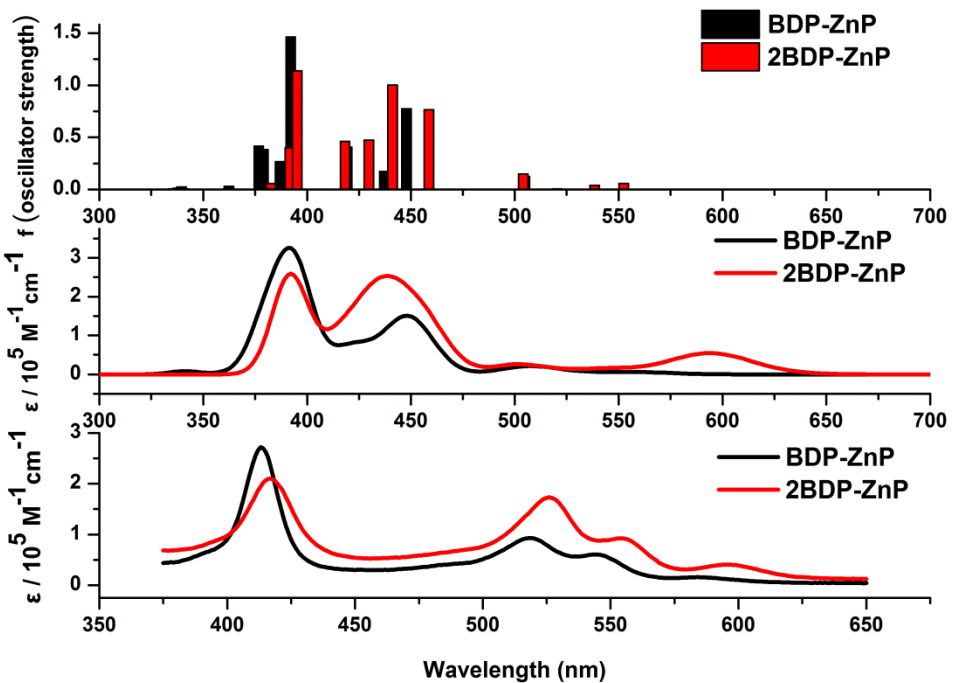


Fig. S7 The oscillator strength of the hybrids (top); simulated spectra from TDDFT calculations at the B3LYP/6-31g* level with Polarizable Continuum Model (middle); absorption spectra in CHCl₃ (bottom). The simulated spectra were generated using a 1300 cm⁻¹ half bandwidth.

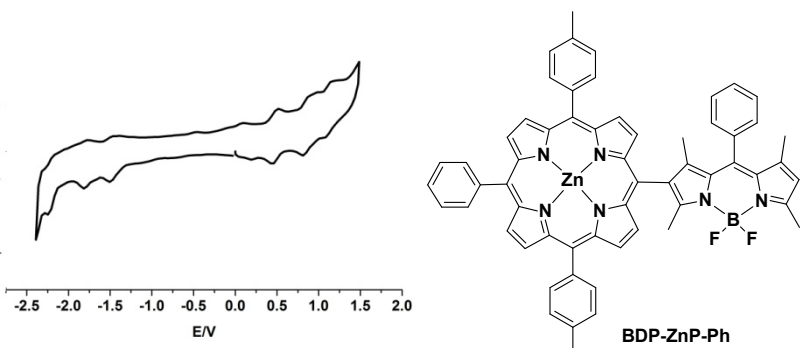


Fig. S8 Cyclic voltammogram of the hybrid BDP-ZnP-Ph in benzonitrile. The voltages are vs. the saturated calomel electrode (SCE).

Table S3 Redox data vs. Fc/Fc⁺ in benzonitrile^a

compound	$E_{1/2}^{\text{Ox1}}/\text{V}(\Delta E_p/\text{V})$	$E_{1/2}^{\text{Ox2}}/\text{V}$	$E_{1/2}^{\text{Ox3}}/\text{V}$	$E_{1/2}^{\text{Red1}}/\text{V}$	$E_{1/2}^{\text{Red2}}/\text{V}$
BDP-ZnP	0.42(0.08)	0.82(0.15)	1.04(0.08)	-1.54(0.07)	-1.89(0.07)
BDP-ZnP-Ph	0.33(0.07)	0.72(0.07)		-1.61(0.08)	-1.92(0.08)
2BDP-ZnP	0.32(0.06)	0.63(0.06)		-1.62(0.07)	-1.99(0.07)
4BDP-ZnP	0.35(0.06)	0.64(0.06)		-1.63(0.07)	-2.17(0.07)

^a Using 0.1 M *n*-Bu₄NPF₆ as supporting electrolyte.

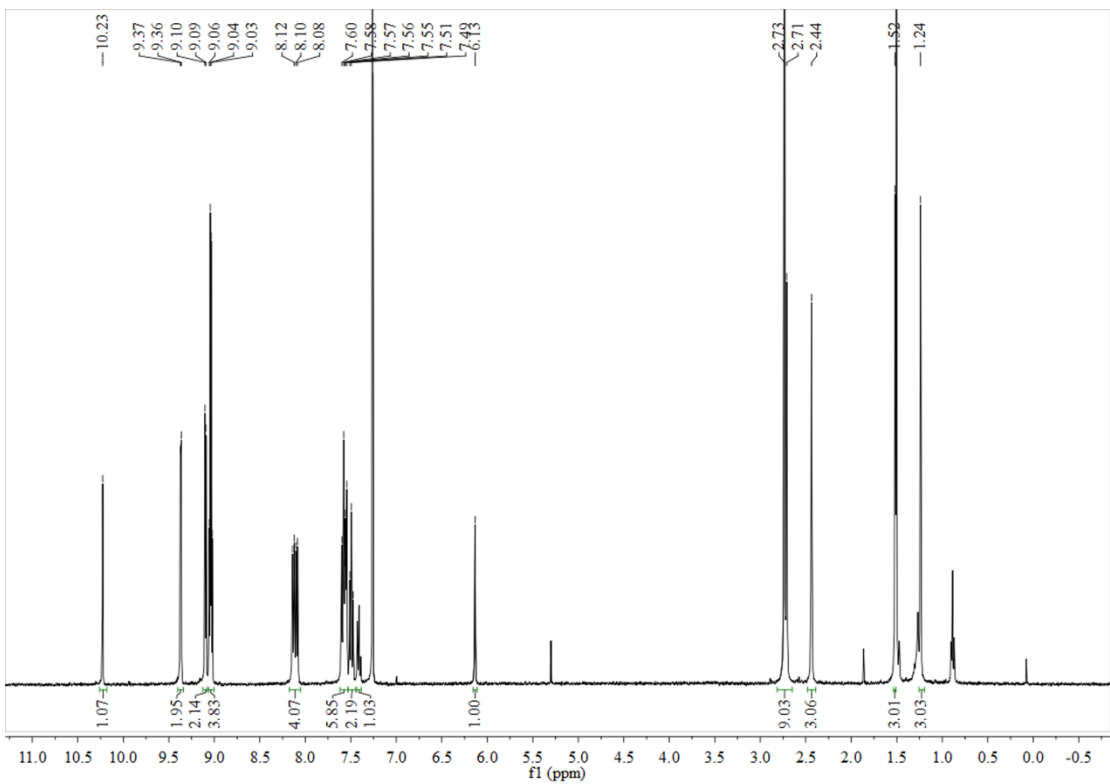


Fig. S9 ^1H NMR spectra of **BDP-ZnP** in CDCl_3 .

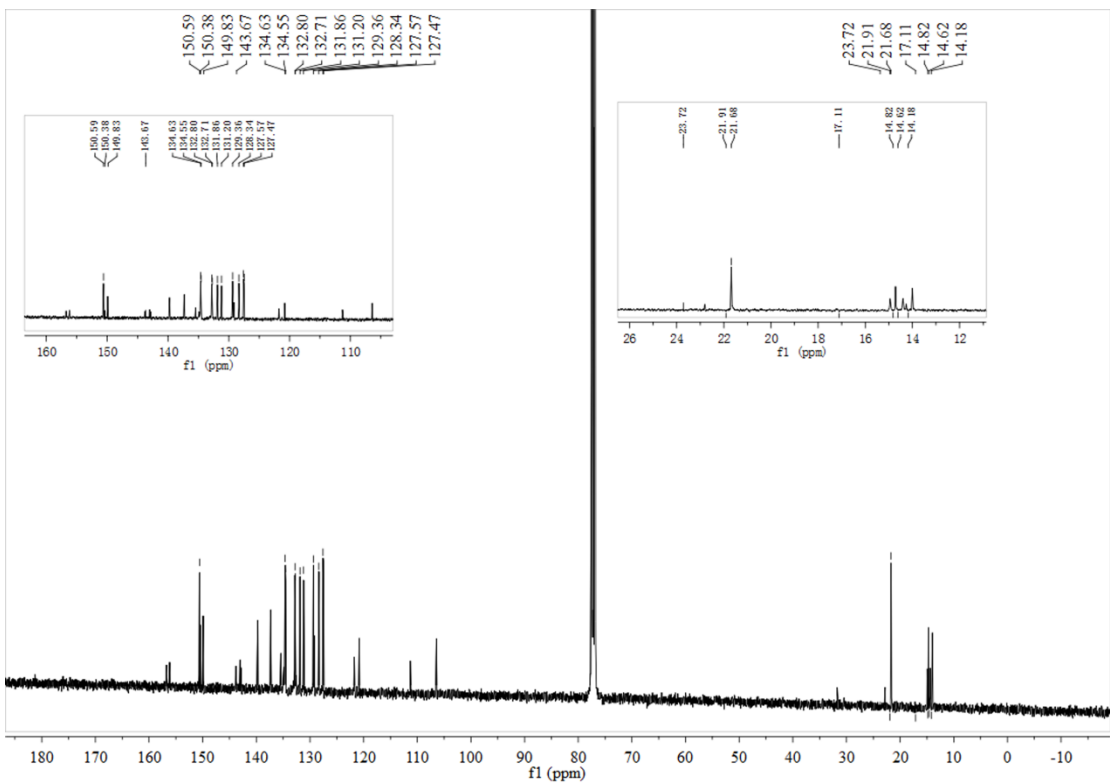


Fig. S10 ^{13}C NMR spectra of **BDP-ZnP** in CDCl_3 .

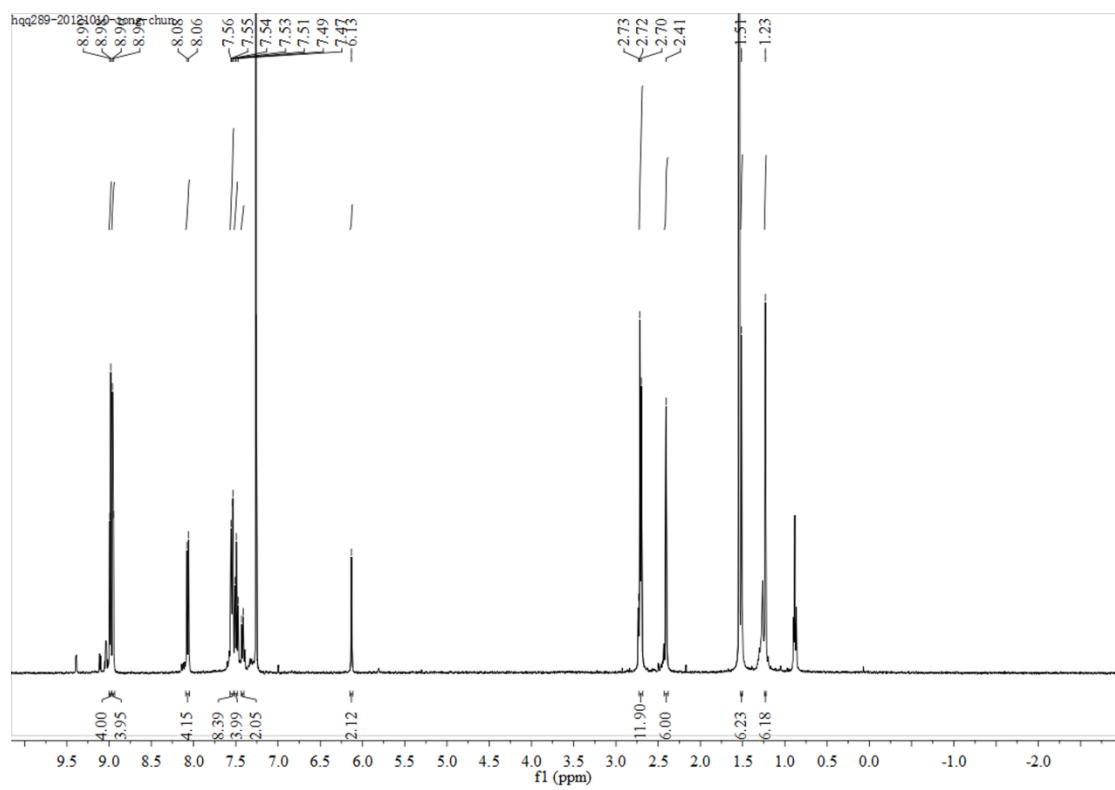


Fig. S11 ^1H NMR spectra of **2BDP-ZnP** in CDCl_3 .

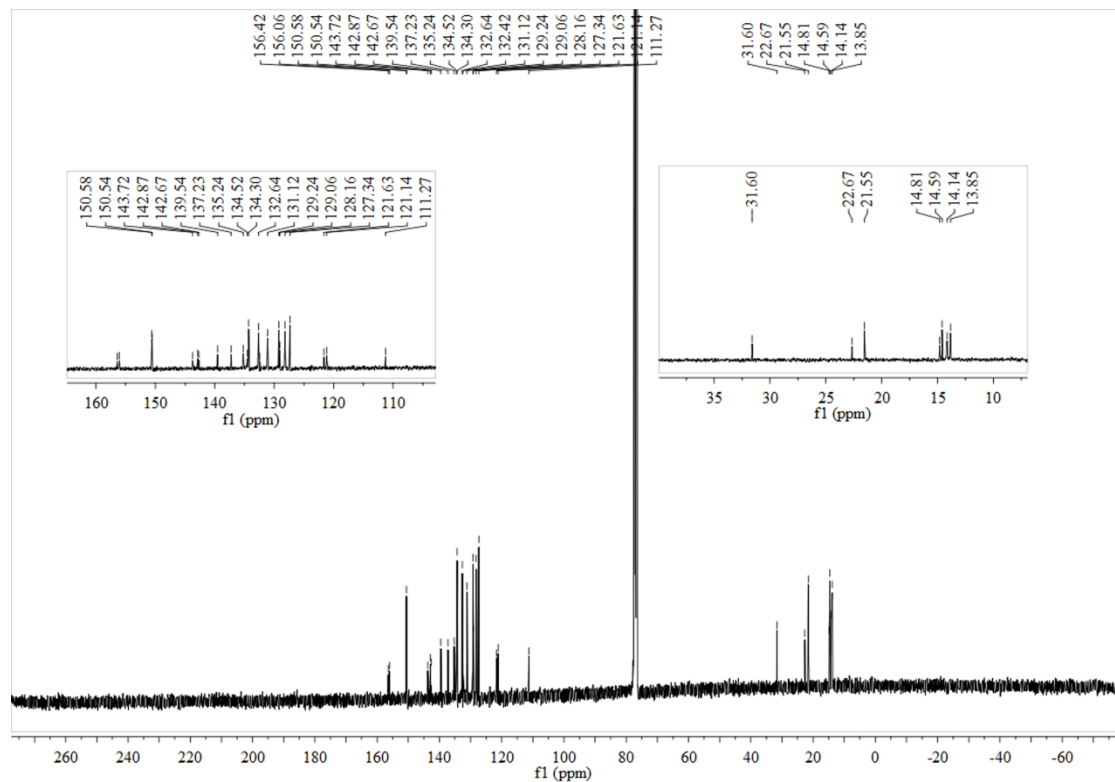


Fig. S12 ^{13}C NMR spectra of **2BDP-ZnP** in CDCl_3 .

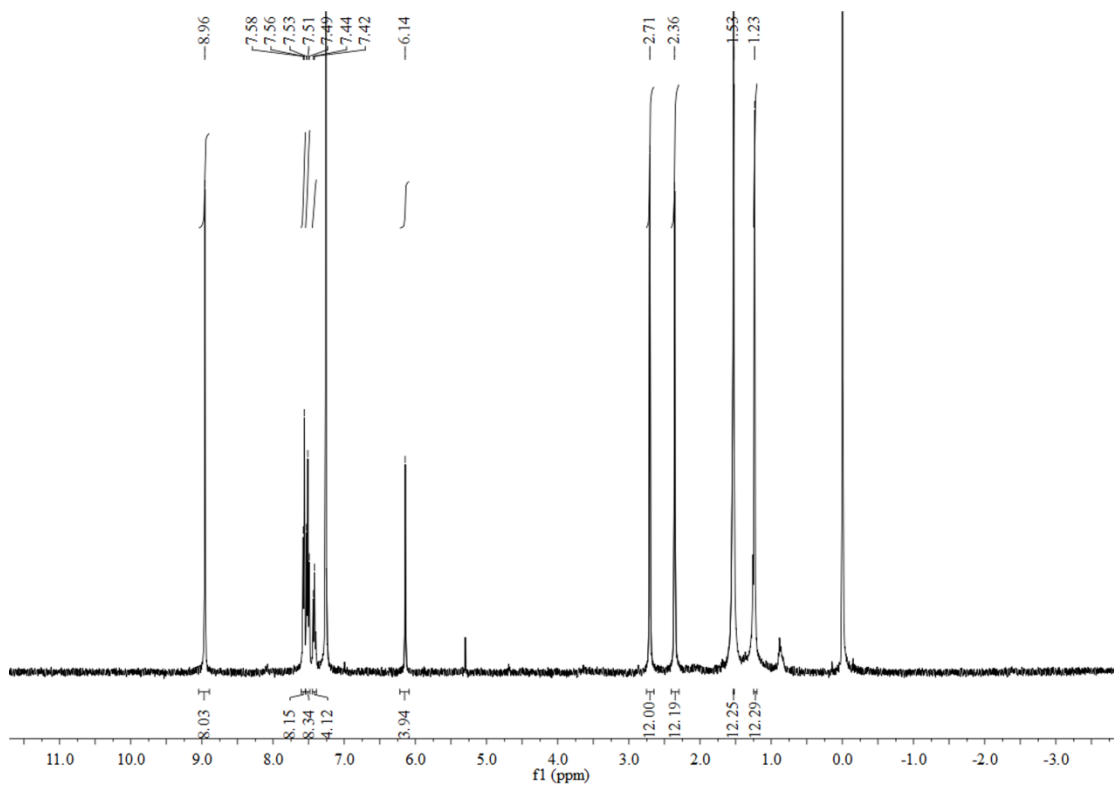


Fig. S13 ^1H NMR spectra of **4BDP-ZnP** in CDCl_3 .

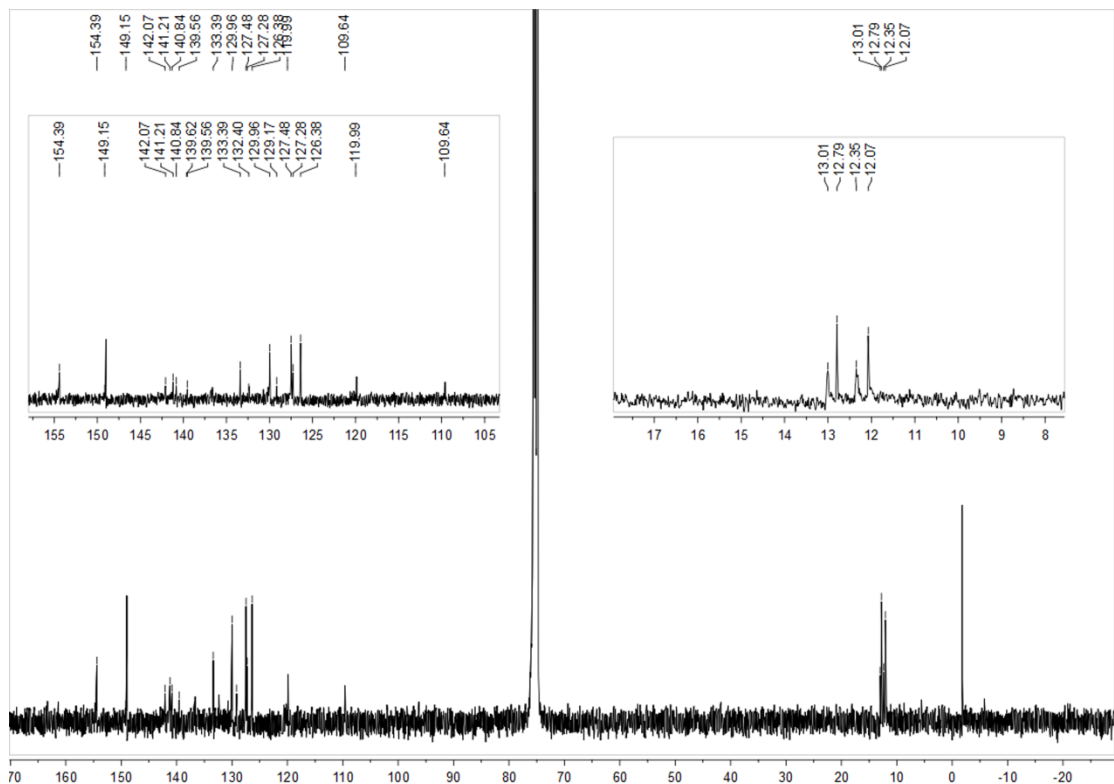


Fig. S14 ^{13}C NMR spectra of **4BDP-ZnP** in CDCl_3 .

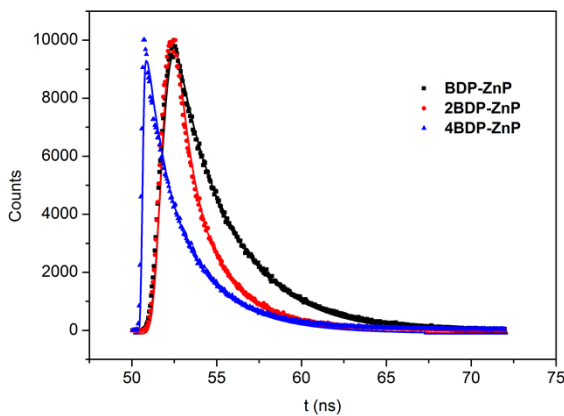


Fig. S15 Fluorescence decays of **BDP-ZnP**, **2BDP-ZnP**, and **4BDP-ZnP** measured at the emission wavelength of a BODIPY moiety at 500 nm in toluene. (The pump wavelength is 450 nm)

Table S4 The fitted parameters of fluorescence decays of **BDP-ZnP**, **2BDP-ZnP**, and **4BDP-ZnP**

BDP-ZnP	2BDP-ZnP	4BDP-ZnP
The fitted parameters are:	The fitted parameters are:	The fitted parameters are:
Hi reduced to: 1459	Hi reduced to: 1428 ch	Hi reduced to: 1223 ch
SHIFT = -0.918488 ch	SHIFT = -0.3877274 ch	SHIFT = 0.1118074 ch
-5.04E-11 se	-2.127448E-11 sec	6.134837E-12 sec
S.Dev = 1.90E-12 sec	S.Dev = 2.05895E-12 sec	S.Dev = 1.2195E-12 sec
T1 = 16.29131 ch	T1 = 17.17201 ch	T1 = 17.51223 ch
8.94E-10 sec	9.42223E-10 sec	9.608906E-10 sec
S.Dev = 8.11E-11 sec	S.Dev = 2.974499E-11 sec	S.Dev = 6.989673E-11 sec
T2 = 62.5871 ch	T2 = 51.07912 ch	T2 = 51.84645 ch
3.43E-09 sec	2.802695E-09 sec	2.844798E-09 sec
S.Dev = 7.05E-12 sec	S.Dev = 1.465996E-11 sec	S.Dev = 1.854321E-11 sec
A = -0.6643689	A = 1.518847	A = 0.5308534
S.Dev = 0.1976786	S.Dev = 0.1688163	S.Dev = 0.2520007
B1 = 1.15E-02	B1 = 0.0572117	B1 = 0.1079147
[5.01 Rel.Ampl]	[37.38 Rel.Ampl]	[21.42 Rel.Ampl]
S.Dev = 2.68E-04	S.Dev = 2.69689E-04	S.Dev = 9.493722E-04
B2 = 0.0565997	B2 = 3.222698E-02	B2 = 0.1336813
[94.99 Rel.Ampl]	[62.62 Rel.Ampl]	[78.58 Rel.Ampl]
S.Dev = 9.48E-05	S.Dev = 9.672782E-05	S.Dev = 3.72405E-04
CHISQ = 1.107627	CHISQ = 2.027229	CHISQ = 3.34269
[544 degrees of freedom]	[514 degrees of freedom]	[318 degrees of freedom]
Chi-squared Probability = 4.14%	Chi-squared Probability = 1.9288E-20%	Chi-squared Probability = 1.9288E-20%
Durbin-Watson Parameter = 2.0041	Durbin-Watson Parameter = 1.175693	Durbin-Watson Parameter = 0.7542565
Negative residuals = 45.27%	Negative residuals = 39.61538%	Negative residuals = 47.53086%
Residuals < 1 s.dev = 52.12%	Residuals < 1 s.dev = 52.11538%	Residuals < 1 s.dev = 47.53086%
Residuals < 2 s.dev = 84.62%	Residuals < 2 s.dev = 84.61539%	Residuals < 2 s.dev = 76.23457%
Residuals < 3 s.dev = 96.54%	Residuals < 3 s.dev = 96.53846%	Residuals < 3 s.dev = 90.74074%

Residuals < 4 s.dev = 99.42% Residuals < 4 s.dev = 99.42308% Residuals < 4 s.dev = 97.22222%

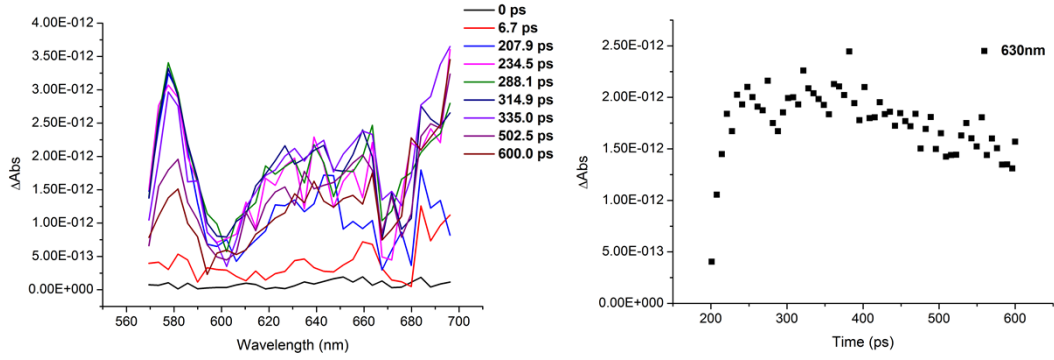


Fig. S16 (Left) Femtosecond transient absorption spectra of BDP-ZnP in benzonitrile ($\lambda_{\text{ex}} = 400$ nm). (Right) The time profile at 630 nm.

Förster theory used in the theoretical calculation:

We have calculated the energy transfer rate and efficiency of energy transfer between BODIPY and ZnP units by Förster theory.^{5, 6}

The transition moment of BODIPY takes a long axis orientation from one pyrrole ring to the other one. This is parallel to one of the two transition moments of porphyrin which are perpendicular to each other, resulting in a higher orientation factor k^2 value ($k^2 = 4$) by using the Equation 1. The overlap integral (J) is relevant to the overlap degree of donor's emission spectra (BODIPY) and the acceptor's absorption spectra (ZnTPP), which is calculated to be $1.65 \times 10^{15} \text{ M}^{-1}\text{cm}^{-1}\text{nm}^4$. Subsequently, the R_0^6 value was estimated to be $1.08 \times 10^{11} \text{ \AA}^6$, and R_0 was about 69.0 Å. The distance (r_{DA}) between the BODIPY and ZnP units in the hybrids is about 8.7 Å. The k_{ET} obtained by Equation 4 was about $5.9 \times 10^{12} \text{ s}^{-1}$, and the $E_{\text{FRET}} > 99.9\%$. The experimental k_{EXP} is close but one order of magnitude smaller than the theoretical value.⁷

$$k^2 = (\sin\theta_D \sin\theta_A \cos\Phi - 2 \cos\theta_D \cos\theta_A)^2 \quad \text{eq 1}$$

$$J = \frac{\theta_D = \theta_A = 0^\circ}{\int_0^\infty F_D(\lambda) \varepsilon_\lambda(\lambda) \lambda^4 d\lambda} \quad \text{eq 2}$$

$$R_0^6 = 8.79 \times 10^{-5} \left(\frac{\Phi_D k^2}{n^4} \right) \times J \quad \text{eq 3}$$

$$k_{\text{ET}} = \frac{R_0^6}{\tau_D r_{\text{DA}}^6} \quad \text{eq 4}$$

$$E_{\text{FRET}}(\%) = \left[\frac{R_0^6}{R_0^6 + r_{\text{DA}}^6} \right] \times 100\% \quad \text{eq 5}$$

Dexter mechanism used in the theoretical calculation:

We have used the Dexter mechanism to evaluate the possibility of through-bond energy transfer in the hybrids.⁸

The frontier orbitals from DFT calculation show obvious overlaps between BODIPY and Zn porphyrin, especially in the hybrids **2BDP-ZnP** and **4BDP-ZnP**. This may allow Dexter mechanism to compete with Forster. According to Equation 6, the overlap integral (J_D), which is relevant to the overlap degree of donor's emission spectra (BODIPY) and the acceptor's absorption spectra (ZnTPP), was calculated to be 2.44 eV^{-1} . Subsequently, the intercomponent electronic interaction parameter (H) was calculated to be 17.5 cm^{-1} by Equation 7 using the experimentally obtained energy transfer rate of $1.1 \times 10^{11} \text{ s}^{-1}$ (k_D of **4BDP-ZnP**).⁵ Considering the obvious orbital overlaps between **BDP** and **ZnP** from DFT theoretical calculation, this somewhat big H value seems to be reasonable. Also, using the values of J_D and k_D , the parameter KJ_D in Equation 7 was calculated to be $2.59 \times 10^{-17} \text{ erg}$, which is about 2 orders of magnitude higher than that reported energy transfer via exchange interaction in bichromophoric molecules ($KJ_D = 2.33 \times 10^{-12} \text{ dyn} * 2 \times 10^{-7} = 4.66 \times 10^{-19} \text{ erg}$).^{9,10} Thus, the photoinduced energy transfer in our hybrids may not be controlled by the Dexter mechanism.

$$J_D = \int_0^{\infty} F_D(\bar{v}) \bar{\epsilon}_A(\bar{v}) d\bar{v} \quad \text{eq 6}$$

and

$$J = \int_0^{\infty} F_D(\bar{v}) d\bar{v} = 1 \quad J = \int_0^{\infty} \bar{\epsilon}_A(\bar{v}) d\bar{v} = 1$$

$$k_D = \frac{4\pi^2 H^2}{h} J_D = \frac{4\pi^2 K}{h} J_D \exp\left(-\frac{2R}{L}\right) \quad \text{eq 7}$$

References

1. J. P. Collman, R. R. Gagne, C. A. Reed, T. R. Halbert, G. Lang, W.T. Robinson, *J. Am. Chem. Soc.*, 1975, **97**, 1427–1439.
2. K. Hatano, K. Anzai, T. Kubo, S. Tamai, *Bull. Chem. Soc. Jpn.*, 1981, **54**, 3518–3521.
3. L. R. Milgrom, P. J. F. Dempsey, G. Yahioglu, *Tetrahedron*, 1996, **52**, 9877–9890.
4. K. Anzai, K. Hatano, *Chem. Pharm. Bull.*, 1984, **32**, 1273–1278.
5. T. Lazarides, G. Charalambidis, A. Vuillamy, M. Réglier, E. Klontzas, G. Froudakis, S. Kuhri, D. M. Guldin, A. G. Coutsolelos, *Inorg. Chem.*, 2011, **50**, 8926–8936.
6. J.R. Lakowicz, *Principles of Fluorescence Spectroscopy*, 2nd ed.; Kluwer / Plenum: New York, 1999.
7. H. S. Cho, D. H. Jeong, M.-C. Yoon, Y. H. Kim, Y.-R. Kim, and D. Kim, *J. Phys. Chem. A*, 2001, **105**, 4200–4210.
8. D. L. Dexter, *J. Chem. Phys.*, 1953, **21**, 836–850.
9. S. Hassoon, H. Lustig, M. B. Rubin and S. Speiser, *J. Phys. Chem.*, 1984, **88**, 6367–6374.
10. B. Pispisa, A. Palleschi, L. Stella, M. Venanzi, C. Mazzuca, F. Formaggio, C. Toniolo and Q. B. Broxterman, *J. Phys. Chem., B* 2002, **106**, 5733–5738.